Oncology Research, Vol. 28, pp. 147–159
Printed in the USA.

0965-0407/20 $90.00 + .00
DOI: https://doi.org/10.3727/096504019X15732109856009
E-ISSN 1555-3906
www.cognizantcommunication.com

MicroRNA-561 Affects Proliferation and Cell Cycle Transition Through PTEN/AKT Signaling Pathway by Targeting P-REX2a in NSCLC

ZiJun Liao,*† Qi Zheng,† Ting Wei,‡ YanBing Zhang,† JieQun Ma,† Zheng Zhao,§ HaiFeng Sun,§ and KeJun Nan*

*Department of Medical Oncology, The First Affiliated Hospital of Xi'an Jiaotong University, Xi'an, Shaanxi Province, P.R. China
†First Department of Medical Oncology, Affiliated Shaanxi Provincial Cancer Hospital, College of Medicine, Xi'an Jiaotong University, Shaanxi Province, P.R. China
‡Department of Ophthalmology, The First Affiliated Hospital of Xi'an Jiaotong University, Xi'an, Shaanxi Province, P.R. China
§Third Department of Medical Oncology, Affiliated Shaanxi Provincial Cancer Hospital, College of Medicine, Xi'an Jiaotong University, Shaanxi Province, P.R. China

MicroRNAs (miRNAs) play crucial roles in tumorigenesis and tumor progression. miR-561 has been reported to be downregulated in gastric cancer and affects cancer cell proliferation and metastasis. However, the role and underlying molecular mechanism of miR-561 in human non-small cell lung cancer (NSCLC) remain unknown and need to be further elucidated. In this study, we discovered that miR-561 expression was downregulated in human NSCLC tissues and cell lines. The overexpression of miR-561 inhibited NSCLC cell proliferation and cell cycle G_1/S transition and induced apoptosis. The inhibition of miR-561 facilitated cell proliferation and G_1/S transition and suppressed apoptosis. miR-561 expression was inversely correlated with P-REX2a expression in NSCLC tissues. P-REX2a was confirmed to be a direct target of miR-561 using a luciferase reporter assay. The overexpression of miR-561 decreased P-REX2a expression, and the suppression of miR-561 increased P-REX2a expression. Particularly, P-REX2a silencing recapitulated the cellular and molecular effects observed upon miR-561 overexpression, and P-REX2a overexpression counteracted the effects of miR-561 overexpression on NSCLC cells. Moreover, both exogenous expression of miR-561 and silencing of P-REX2a resulted in suppression of the PTEN/AKT signaling pathway. Our study demonstrates that miR-561 inhibits NSCLC cell proliferation and G_1/S transition and induces apoptosis through suppression of the PTEN/AKT signaling pathway by targeting P-REX2a. These findings indicate that miR-561 plays a significant role in NSCLC progression and serves as a potential therapeutic target for NSCLC.

Key words: miR-561; P-REX2a; Non-small cell lung cancer (NSCLC), Proliferation; Cell cycle; Apoptosis

INTRODUCTION

Lung cancer is the first leading cause of death worldwide, influencing up to 31% of males and 27% of females[1]. Non-small cell lung cancer (NSCLC) and small cell lung cancer account for approximately 85% and 15% of all lung cancers, respectively[2]. Despite advances in detection and improvements to standard of care, NSCLC is often diagnosed at an advanced stage and bears poor prognosis. Recrudescence is frequent after primary and adjuvant therapy, often evolving into a lethal metastatic disease[3]. Tumorigenesis and development are the polyfactorial and multistep processes involving different gene changes, including the inactivation of tumor suppressor genes, activation of oncogenes, and abnormal expression of cancer-related genes[4]. Therefore, it is critical to uncover the molecular mechanisms underlying NSCLC development and progression, which could reveal novel biomarkers and support the development of therapeutic strategies for patients with NSCLC.

MicroRNAs (miRNAs) are a family of endogenous, single-stranded, small noncoding RNA molecules of approximately 23 nucleotides that act as crucial regulators of gene expression by binding to the 3 -untranslated regions (3 -UTRs) of target mRNAs[5–7]. miRNAs can

Address correspondence to KeJun Nan, Department of Medical Oncology, The First Affiliated Hospital of Xi'an Jiaotong University, 277 West Yanta Road, Xi'an, Shaanxi Province 710061, P.R. China. Tel: +86-29-85324785; Fax: +86-29-85324785; E-mail: qilizi@sohu.com

regulate gene expression by inhibiting translation or accelerating the degradation of mRNA[8]. By regulating different target genes, miRNAs play key roles in diverse biological processes, such as cell proliferation, survival, differentiation, apoptosis, adhesion, tumor angiogenesis, glucose uptake, metastasis, and resistance to cancer chemotherapy[9–13]. miRNAs can downregulate multiple target genes, including oncogenes and tumor suppressors; hence, some miRNAs function as tumor suppressors and others function as oncogenes[14]. Accumulating evidence has revealed that the dysregulation of miRNAs plays a crucial role in NSCLC progression. Recently, it was reported that miR-561 is clinically significant and plays an important role in gastric cancer progression[15]. Nevertheless, the role and molecular mechanism of miR-561 in human NSCLC development remain unknown and need to be further elucidated.

In this study, we found that the expression of miR-561 was significantly downregulated in NSCLC tissues and correlated with clinicopathological characteristics, such as TNM stage and tumor size. In addition, the results showed that phosphatidylinositol 3,4,5-trisphosphate RAC exchanger 2a (P-REX2a) was overexpressed in NSCLC tissues. We predicted that miR-561 could target P-REX2a by using bioinformatics software (miRBase). P-REX2a is a guanine nucleotide exchange factor for the RAC guanosine triphosphatase, playing a PTEN-interacting protein, which can activate the phosphoinositide 3-kinase (PI3K) signaling pathway by antagonizing PTEN in cancer cells[16]. Furthermore, miR-561 dramatically suppressed human NSCLC cell proliferation and induced G_1/S cell cycle arrest and cell apoptosis. For the first time, we provide evidence that P-REX2a is a direct functional target of miR-561. Our findings suggest that miR-561 may be a novel therapeutic target in NSCLC therapy.

MATERIALS AND METHODS

Human Clinical Samples and Cell Lines

Sixty-eight NSCLC tissues and paired adjacent normal tissues were obtained from patients who were diagnosed in the Department of Oncological Surgery, First Affiliated Hospital, Xi'an Jiaotong University, China. We obtained informed consent from each patient before specimen collection. The tissues were immediately frozen and stored at −80°C. The experiments were approved by the Ethics Committee of Xi'an Jiaotong University Health Science Center. Human NSCLC cell lines (NCI-H460, A549, and NCI-H292) and normal human bronchial epithelial cells (BEAS-2B) were purchased from the Cell Bank (Chinese Academy of Sciences, Shanghai, P.R. China). These cells were maintained in Dulbecco's modified Eagle's medium (DMEM; Gibco BRL, Grand Island, NY, USA) supplemented with 10% fetal bovine serum (Gibco BRL), penicillin (100 U/ml), and streptomycin (100 µg/ml) and were incubated at 37°C in a humidified atmosphere of 5% CO_2 and 95% air.

Isolation of Total RNA and Quantitative Real-Time PCR (qRT-PCR)

Total RNA was extracted from human NSCLC tissues and cell lines with TRIzol reagent (Thermo Fisher Scientific, Waltham, MA, USA). The SYBR Premix Ex Taq II Kit (Takara, Dalian, P.R. China) was used to detect miR-561 expression and P-REX2a mRNA expression. qRT-PCR was fulfilled using the iCycler iQ Multicolor qRT-PCR System (Bio-Rad Laboratories, Hercules, CA, USA). The data were normalized to RNU6B (U6) or -actin expression. The primer sequences were as follows: miR-561: 5 -GTCGTATCCAGT GCGTGTCGTGGAGTCGGCAATTGCACTGGATA CGACACTTCAA-3 (reverse transcribed); miR-561: 5 -ATCCAGTGCGTGTCGTG-3 (forward) and 5 -TGCT CAAAGTTTAAGATCC-3 (reverse); U6: 5 -CGCTT CACGAATTTGCGTGTCAT-3 (reverse transcribed), 5 -GCTTCGGCAGCACATATACTAAAAT-3 (forward), and 5 -CGCTTCACGAATTTGCGTGTCAT-3 (reverse); P-REX2a: 5 -AACCATGAGAAGGCACAAAAA-3 (forward) and 5 -CTTGCATATTCTTTGTATTGGTGT-3 (reverse); -actin: 5 -TGGCACCCAGCACAATGAA-3 (forward) and 5 -CTAAGTCATAGTCCGCCTAGAA GCA -3 (reverse).

Western Blotting

We conducted the experiment according to the standard method. Briefly, samples and NSCLC cells were lysed using lysis buffer (Wolsen Biotech, Xi'an, P.R. China) and centrifuged at 12,000 × *g*. The protein concentration was measured with the bicinchoninic acid (BCA) assay. The total protein was separated through 10% SDS-PAGE and electrophoretically transferred onto PVDF membranes (Invitrogen, Carlsbad, CA, USA). Then the membrane was incubated for 1 h in blocking solution containing 5% nonfat dry milk and incubated with primary antibodies overnight at 4°C. The primary antibodies were as follows: mouse polyclonal anti-P-Rex2a (1:1,000; Cell Signaling Technology, Danvers, MA, USA), rabbit monoclonal anti-PTEN (1:1,000; Santa Cruz Biotechnology, Santa Cruz, CA, USA), rabbit monoclonal anti-p-AKT (1:1,000; Santa Cruz Biotechnology), rabbit monoclonal anti-AKT (1:2,000; Santa Cruz Biotechnology), mouse monoclonal anti-cyclin D1 (1:1,000; Santa Cruz Biotechnology), mouse monoclonal anti-CDK2 (1:1,000; Santa Cruz Biotechnology), rabbit monoclonal anti-Bcl-2 (1:1,000; Santa Cruz Biotechnology), rabbit monoclonal anti-Bax (1:1,000; Santa Cruz Biotechnology), anti-caspase 9 (1:1,000; Santa Cruz Biotechnology), anti-caspase 3 (1:1,000; Santa Cruz Biotechnology), and

mouse monoclonal anti- -actin (1:4,000; Santa Cruz Biotechnology). The blots were developed with an ECL chemiluminescence kit (Pierce, Rockford, IL, USA). The blots were scanned, and the band densities were analyzed using PDQuest software.

Immunofluorescence

For immunofluorescent staining, A549 cells were fixed with chilled methanol and acetone and then blocked with 10% normal goat serum in PBS containing 0.3% Triton X-100 for 1 h at room temperature. Mouse polyclonal anti-P-Rex2a (1:100; Cell Signaling Technology) was diluted in PBS containing 3% bovine serum albumin. Cells were incubated with anti-P-Rex2a antibody at 4°C overnight and were then washed with PBS for 5 min three times. Subsequently, the anti-mouse IgG–FITC (1:1,000; Santa Cruz Biotechnology) was added, followed by 2 h of incubation. Negative controls lacking the primary antibody were used to eliminate nonspecific staining. Immunostained cells were visualized by indirect fluorescence under a fluorescent microscope (Olympus BX51; Olympus, Tokyo, Japan) equipped with a DP70 digital camera and the DPManager (DPController) software (Olympus).

Anti-miR-561 and P-REX2a siRNA Transfection

Interfering RNA oligonucleotides served as miR-561 inhibitors (named anti-miR-561) and were synthesized by Gene Pharma (Shanghai, P.R. China). The sequence of anti-miR-561 was 5 -ACUUCAAGGAUCUUAAAC UUUG-3 . Scramble siRNA was used as a control (named anti-miR-Control), and the sequence was 5 -CAGUAC UUUUGUGUAGUACAA-3 . The inhibitors were transfected into human NSCLC A549 cells with Lipofectamine 2000. Small interfering RNA (siRNA) was used to silence the human P-REX2a gene. P-REX2a siRNA (sense 5 -CACUAUGGCCAUCAUUGAUTT-3 , antisense 5 -AU CAAUGAUGGCCAUAGUGTT-3) and negative siRNA (NC-siRNA, sense 5 -UUCUCCGAACGUGUCACGU TT-3 , antisense 5 -ACGUGACACGUUCGGAGAATT-3) were transfected using Lipofectamine 2000 and diluted to a concentration of 60 nM for use in future experiments in A549 cells.

Expression Vector Construction

The Hsa-miR-561 precursor expression vector (named miR-561) and the control empty vector (named control) were constructed with synthetic oligonucleotides and incorporated into the pcDNA6.2-GW/EmGFPmiR plasmid according to the manufacturer's instructions. Full-length human P-REX2a complementary DNA was cloned into the pCMV2-GV146 vector. Transfection was fulfilled using Lipofectamine 2000 (Invitrogen) according to the manufacturer's instructions.

Dual-Luciferase Assay

The binding site for miR-561 in the 3 -UTR of P-REX2a was constructed with synthetic oligonucleotides (AuGCT DNA-SYN Biotechnology, Beijing, P.R. China) and cloned into the pmirGLO Dual-Luciferase expression vector (named P-REX2a-WT). The mutated 3 -UTR sequences of P-REX2a were also cloned and named P-REX2a-MT. The pre-miR-561 expression vector and the WT or MT reporter plasmids were cotransfected into HEK293T cells. The cells were collected 24 h after transfection. The Dual-Luciferase Assay System (Promega, Madison, WI, USA) was used to examine reporter activity.

MTT Assay

Human NSCLC A549 cells were seeded into three 96-well plates (four parallel wells/group) and cultured for 24 h. The cells were treated with control, miR-561, anti-miR-Control, anti-miR-561, NC-siRNA (60 nM), P-REX2a siRNA (60 nM), empty vector control, and the P-REX2a overexpression vector for 24, 48, and 72 h, respectively. Cell viability was measured with the MTT assay on a Versamax microplate reader (Molecular Devices, Sunnyvale, CA, USA) at a wavelength of 492 nm.

Cell Counting Assay

To examine cell proliferation, 2.5×10^5 cells were plated in 60-mm-diameter plates and cultured for 24 h. A549 cells were treated separately with control, miR-561, anti-miR-control, anti-miR-561, NC-siRNA (60 nM), P-REX2a siRNA (60 nM), vector control, and the P-REX2a overexpression vector. The number of cells was counted at 24, 48, and 72 h after treatment with a Countess automated cell counter (Life Technologies Corp., Carlsbad, CA, USA).

Cell Cycle Analysis

The A549 cells were cultured in six-well plates and treated for 24 h. The cells were harvested and fixed in 70% ice-cold ethanol at 4°C. The fixed cells were washed in PBS and stained with 50 μg/ml propidium iodide and 50 μg/ml RNase A (DNase-free) for 20 min at room temperature. These cells were subjected to fluorescence-activated cell sorting (BD Biosciences, San Diego, CA, USA). Different cell cycle populations were analyzed using ModFit software.

Apoptosis Assay

A549 cells were seeded into six-well plates and treated for 48 h. We detected cell apoptosis with an Annexin-V–FITC Apoptosis Detection kit (BD Biosciences) according to the manufacturer's instructions. Apoptotic cells were examined using a flow cytometer (BD Biosciences). ModFit software was used to analyze apoptotic changes.

Statistical Analysis

All data were analyzed using SPSS 21.0 software (Abbott Laboratories, Chicago, IL, USA). All experiments were performed at least three times independently. The statistical significance of differences between groups was analyzed with one-way ANOVA or Student's *t*-test. Correlation analysis between miR-561 and P-REX2a in NSCLC tissues was performed using Pearson's correlation analysis. The data are presented as the mean ± standard error of the mean (SEM) from three independent experiments. Values of $p < 0.05$ were considered to indicate statistically significant differences.

RESULTS

miR-561 Is Significantly Downregulated in Human NSCLC Tissues and Cell Lines

To analyze the expression status of miR-561 in human NSCLC tissues, we performed qRT-PCR to examine miR-561 expression in clinical samples (68 NSCLC tissues and adjacent normal tissues) and NSCLC cell lines. The qRT-PCR assays showed that miR-561 expression was dramatically lower in NSCLC tissues than in adjacent normal tissues ($p < 0.01$) (Fig. 1A). Subsequently, we investigated the correlations between miR-561 expression and the clinicopathological characteristics of NSCLC patients. As shown in Table 1, low miR-561 expression was associated with TNM stage and tumor size of NSCLC ($p < 0.01$). However, miR-561 expression was not associated with sex, age, differentiation, and metastasis. Furthermore, miR-561 expression was significantly lower in NSCLC cell lines (NCI-H460, A549, and NCI-H292) than in BEAS-2B cells ($p < 0.01$) (Fig. 1B). These results indicated that miR-561 might be an effective biomarker for the diagnosis and detection of NSCLC.

miR-561 Inhibits NSCLC A549 Cell Proliferation, Prohibits Cell Cycle Transition, and Induces Apoptosis

To investigate the role of miR-561 in human NSCLC, A549 cells were transfected with the miR-561 precursor expression vector, a control empty vector, miR-561 antisense oligonucleotides, or the negative control. miR-561 expression was detected by qRT-PCR after transfection. miR-561 expression was remarkably increased in cells transfected with the miR-561 vector compared to that in cells transfected with the control vector ($p < 0.01$); however, there were no prominent differences between the anti-miR-561 group and the anti-miR-Control group (Fig. 2A and B). An MTT assay revealed that miR-561 overexpression significantly suppressed the proliferation of A549 cells at 48 and 72 h after transfection ($p < 0.01$) (Fig. 2C), while anti-miR-561 promoted cell growth at 48 and 72 h after transfection ($p < 0.01$) (Fig. 2D). A similar trend was observed in the cell counting assay. miR-561 overexpression suppressed cell proliferation, but anti-miR-561 promoted cell growth ($p < 0.01$) (Fig. 2E and F). Because cell cycle is involved in the regulation of cell proliferation, we examined this process using a flow cytometer. The results revealed that miR-561 overexpression resulted in a remarkable accumulation of the G_0/G_1 phase population and a reduction of the S and G_2/M phase populations in A549 cells ($p < 0.01$) (Fig. 2G); inhibition of miR-561 significantly decreased the G_0/G_1 phase population and increased the S and G_2/M phase populations ($p < 0.01$) (Fig. 2H). Evaluation of cell apoptosis confirmed that the ratio of early apoptotic to late apoptotic cells was remarkably increased when miR-561 was overexpressed ($p < 0.01$) (Fig. 2I) and clearly decreased when anti-miR-561 was transfected ($p < 0.01$) (Fig. 2J). These findings demonstrated that miR-561 reduced NSCLC

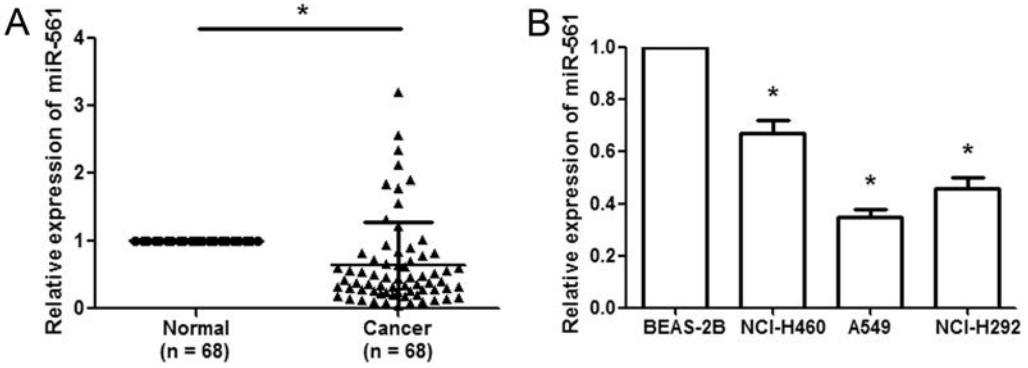

Figure 1. miR-561 is downregulated in non-small cell lung cancer (NSCLC) tissues and cell lines. (A) miR-561 expression was remarkably decreased in NSCLC tissues compared with that in adjacent normal tissues. (B) miR-561 expression was significantly reduced in NSCLC cell lines (NCI-H460, A549, and NCI-H292) compared with that in normal human bronchial epithelial cells (BEAS-2B). Data were analyzed using the $2^{-\Delta\Delta Ct}$ approach. *$p < 0.01$.

Table 1. Clinical Significance of miR-561 Expression in Non-Small Cell Lung Cancer (NSCLC) ($N = 68$)

		miR-561 Expression		
Parameter	All Patients	High ($n = 11$)	Low ($n = 57$)	p Value
Gender				0.781
Male	45	7	35	
Female	23	4	19	
Age				0.768
50 years	37	6	31	
<50 years	31	5	26	
Differentiation				0.183
Moderate-poor	35	5	39	
Well	33	6	27	
Metastasis				0.582
Yes	30	5	25	
No	38	6	32	
Tumor size				0.003*
3 cm	36	3	33	
<3 cm	32	8	24	
TNM stage				0.001*
I + II	30	9	21	
III + IV	38	2	36	

*$p < 0.01$.

cell proliferation and induced G_1/S cell cycle arrest and apoptosis.

P-REX2a Is a Target Gene of miR-561

A bioinformatic database (miRBase) was used to confirm a large number of possible target genes of miR-561. P-REX2a was selected from these candidates for further study. We found that there was a binding site for miR-561 in the 3 -UTR of the P-REX2a mRNA ranging from 3,420 to 3,440 bp (Fig. 3A). To determine whether miR-561 directly targets P-REX2a, a dual-luciferase reporter system containing the WT and MT 3 -UTR of P-REX2a was used. HEK293T cells were cotransfected with reporter plasmids and pre-miR-561 or the pmirGLO empty vector (control). Pre-miR-561/WT-P-REX2a-UTR-transfected cells showed a remarkable reduction in luciferase activity ($p < 0.01$), and pre-miR-561/MT-P-REX2a-UTR-transfected cells failed to exhibit reduced relative luciferase activity (Fig. 3B), suggesting that miR-561 directly targets the 3 -UTR of P-REX2a. Next we measured P-REX2a expression at the mRNA and protein levels. Our results showed that the expression of P-REX2a was significantly upregulated at both the mRNA and protein levels in NSCLC tissues compared to that in adjacent normal tissues ($p < 0.01$) (Fig. 3C and D). The effect of miR-561 on P-REX2a was assessed based on the data obtained from qRT-PCR. A significant negative correlation was identified between P-REX2a and miR-561 ($n = 68$, $r = -0.7004$, $p < 0.001$, Pearson's correlation) (Fig. 3E).

miR-561 Suppresses NSCLC Cell Proliferation, Induces G_1/S Arrest and Apoptosis via the PTEN/AKT Signaling Pathway by Targeting P-REX2a

miR-561 overexpression significantly decreased the mRNA expression of P-REX2a in A549 cells, while anti-miR-561 remarkably increased P-REX2a mRNA expression ($p < 0.001$) (Fig. 4A and B). Immunofluorescent staining results showed that miR-561 overexpression downregulated P-REX2a protein level in A549 cells, and anti-miR-561 upregulated P-REX2a protein level (Fig. 4C). A similar trend was observed for protein levels (Fig. 4D and E). To further investigate the latent molecular mechanisms of miR-561-regulated cell proliferation, cell cycle transition, and apoptosis, we examined the protein levels of the related PTEN/AKT signaling pathway, the G_1 regulator cyclin D1, and caspase 9/3 using Western blot analysis. Our results showed that miR-561 overexpression downregulated p-AKT, cyclin D1, and CDK2 protein expression levels in A549 cells (Fig. 4D). Anti-miR-561 upregulated p-AKT, cyclin D1, and CDK2 protein expression, whereas the protein expression of PTEN and total AKT remained unchanged (Fig. 4E). Moreover, the findings revealed that miR-561 could also inhibit Bcl2 protein expression, and promote Bax and caspase 9/3 protein expression (Fig. 4D and E). These results demonstrated

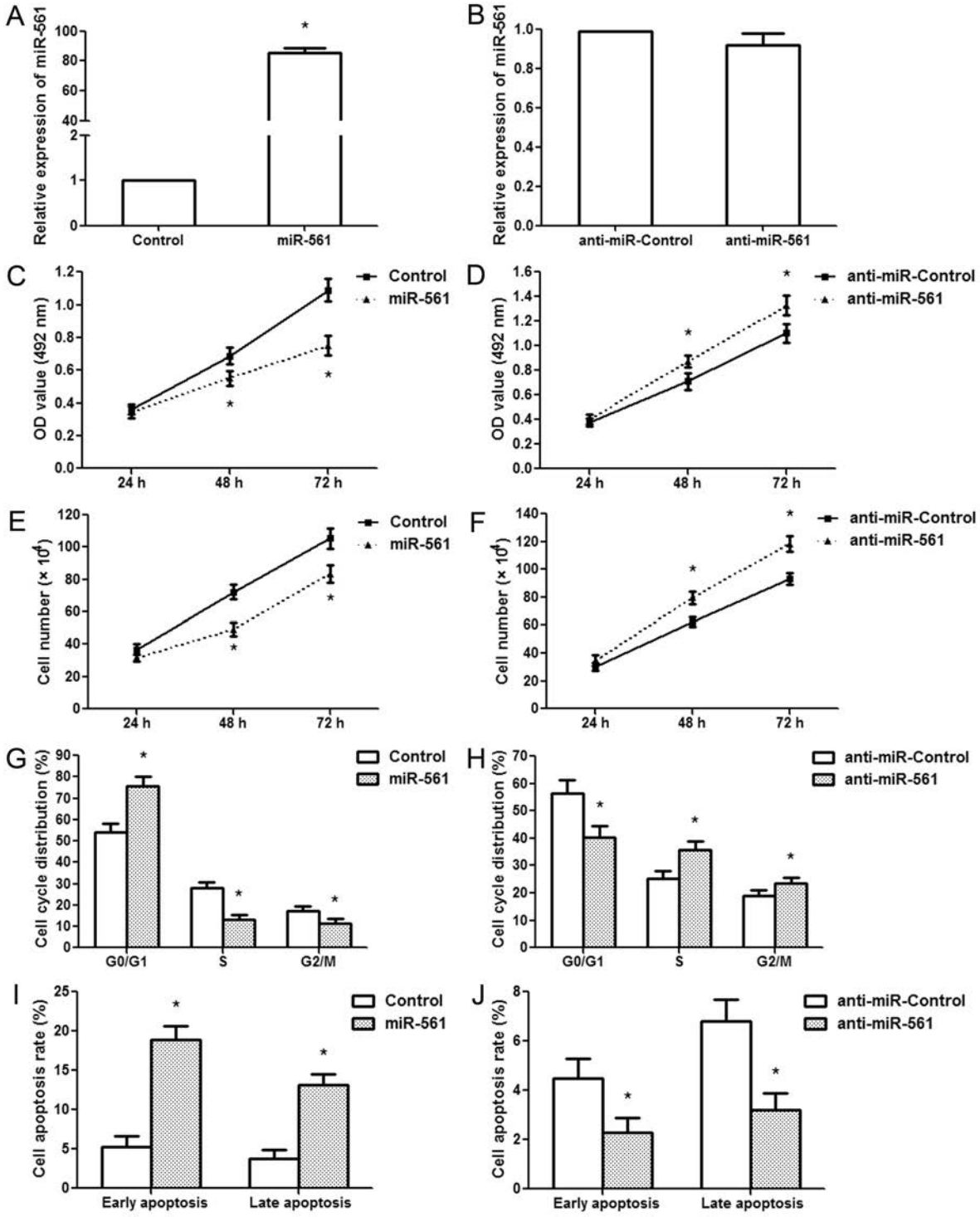

Figure 2. miR-561 suppresses human NSCLC A549 cell proliferation and induces G_1/S cell cycle arrest and apoptosis. (A) miR-561 expression was measured in A549 cells after miR-561 overexpression. (B) miR-561 expression was examined in A549 cells after anti-miR-561 treatment. (C) miR-561 overexpression decreased cell activity at 48 and 72 h after transfection. (D) Anti-miR-561 increased cell activity at 48 and 72 h after transfection. (E) miR-561 overexpression inhibited NSCLC cell proliferation. (F) Anti-miR-561 promoted NSCLC cell growth. (G) The histogram represents the proportion of cells in the G_0/G_1, S, and G_2/M phases after miR-561 overexpression. (H) The ratio of cells in the G_0/G_1, S, and G_2/M phases after anti-miR-561 transfection. (I) The data revealed the ratios of early and late apoptosis after miR-561 overexpression. (J) The data showed the proportions of early apoptosis and late apoptosis after anti-miR-561 transfection. $*p < 0.01$, $n = 3$.

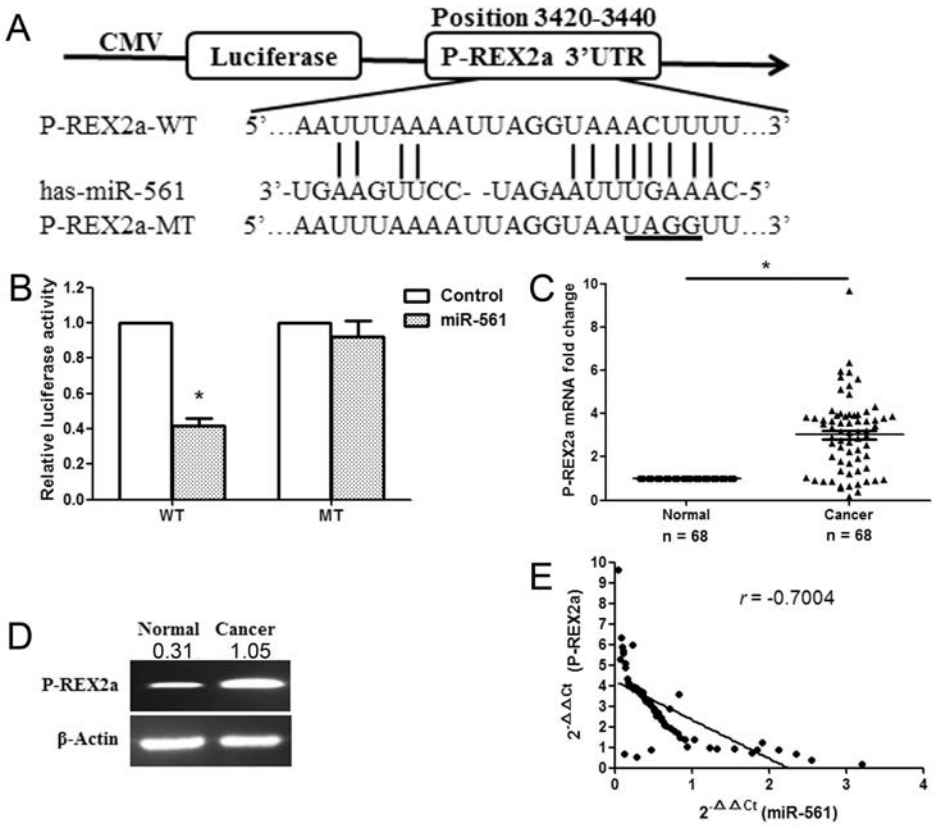

Figure 3. miR-561 directly targets the phosphatidylinositol 3,4,5-trisphosphate RAC exchanger 2a (P-REX2a) gene. (A) Bioinformatics predicted interactions of miR-561 and its binding sites in the 3 -untranslated region (3 -UTR) of P-REX2a. (B) Luciferase activity was detected by the dual-luciferase assay. (C) P-REX2a mRNA expression in human NSCLC tissues. (D) P-REX2a protein levels were measured by Western blotting. (E) miR-561 and P-REX2a levels were inversely correlated. The $2^{-\ Ct}$ values of miR-561 and P-REX2a were subjected to a Pearson correlation analysis ($n = 68$, $r = -0.7004$, $p < 0.001$, Pearson's correlation). *$p < 0.01$.

that miR-561 could modulate NSCLC cell proliferation, the cell cycle via regulating the P-Rex2a/AKT signaling pathway.

Silencing of P-REX2a Restrains NSCLC Cell Proliferation

Since miR-561 regulated cell proliferation, the cell cycle, and apoptosis in NSCLC cells, P-REX2a was validated as a direct target of miR-561; therefore, P-REX2a was knocked down in NSCLC cells by RNA interference to validate its involvement in the tumor suppressor functions of miR-561. Silencing of P-REX2a dramatically decreased cell activity at 48 and 72 h after transfection ($p < 0.01$) (Fig. 5A). A cell counting assay also showed that silencing of P-REX2a remarkably inhibited A549 cell proliferation ($p < 0.01$) (Fig. 5B). Silencing of P-REX2a increased the G_0/G_1 phase population and reduced the S and G_2/M phase populations in A549 cells ($p < 0.01$) (Fig. 5C). Furthermore, silencing of P-REX2a induced apoptosis in A549 cells ($p < 0.01$) (Fig. 5D). Next, we analyzed the knockdown efficiency of P-REX2a siRNA at the mRNA and protein levels. Our results revealed that P-REX2a mRNA and protein expressions were specifically knocked down in A549 cells by the siRNA ($p < 0.01$) (Fig. 5E). The protein expression of P-REX2a decreased significantly in the siRNA group compared with that in the NC-siRNA group, and p-AKT, cyclin D1, CDK2, and Bcl-2 protein expression levels were also reduced, but Bax and caspase 9/3 protein expressions were upregulated (Fig. 5F). These findings were similar to those obtained after miR-561 overexpression, indicating a similar effect of P-REX2a knockdown and miR-561 overexpression.

Overexpression of P-REX2a Counteracted the Effects of miR-561 on NSCLC Cells

To further confirm that miR-561 performed a tumor suppressor function via P-REX2a, we constructed a P-REX2a overexpression vector, which was cotransfected with miR-561 into A549 cells. After cotransfection with the miR-561 and P-REX2a vectors, we found that the overexpression of P-REX2a counterbalanced the tumor suppressor effect of miR-561 in NSCLC cells during cell

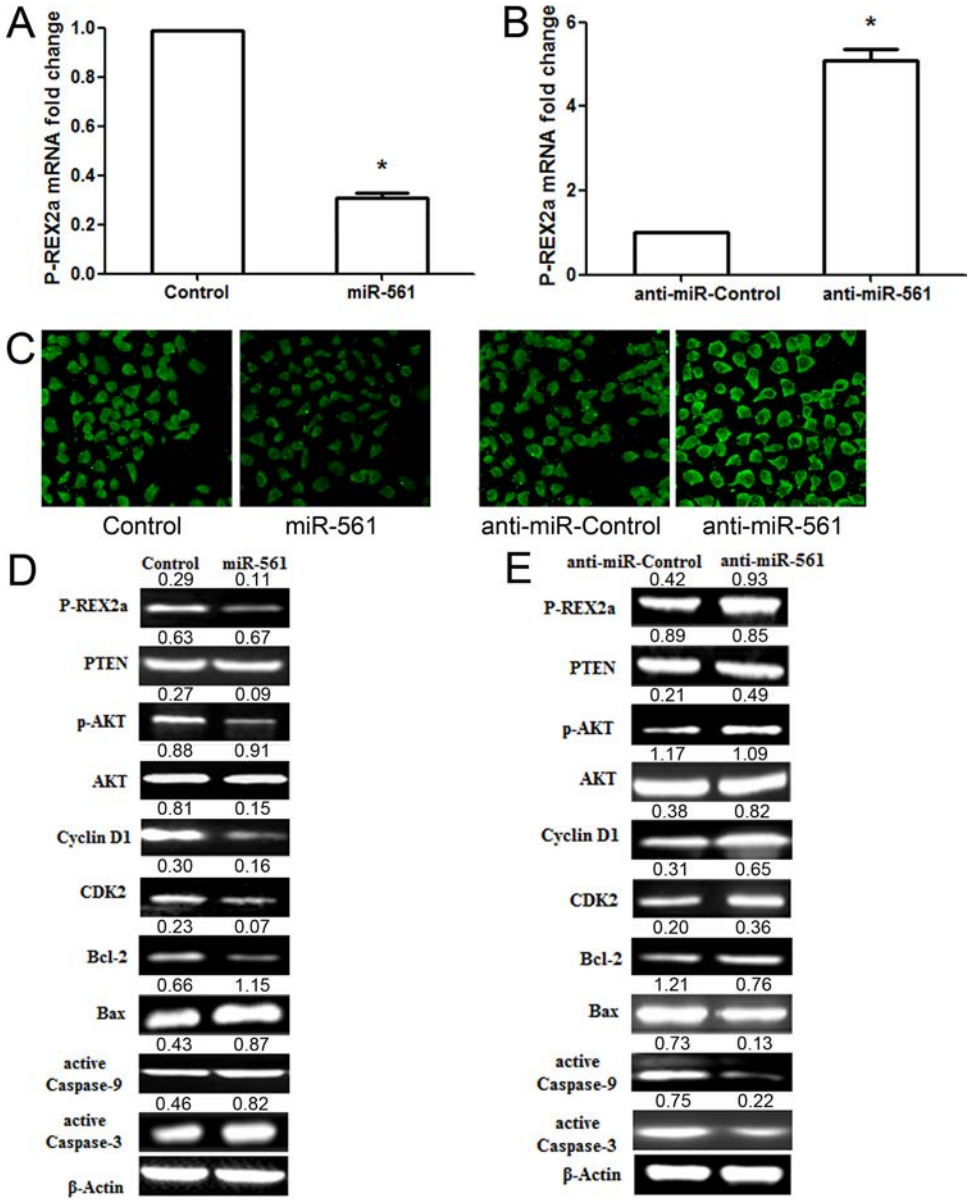

Figure 4. miR-561 regulates the AKT signaling pathway in human NSCLC cells by targeting P-REX2a. (A) P-REX2a mRNA was determined in A549 cells after miR-561 overexpression. (B) P-REX2a mRNA was examined in A549 cells after anti-miR-561 treatment. (C) A549 cells were stained with anti-P-REX2a. (D) miR-561 overexpression inhibited the expressions of the P-REX2a, p-AKT, cyclin D1, CDK2, and Bcl-2 proteins, and promoted Bax and caspase 9/3 expressions in A549 cells. (E) Anti-miR-561 facilitated P-REX2a, p-AKT, cyclin D1, CDK2, and Bcl-2 protein expressions, and decreased Bax and caspase 9/3 expressions. $*p < 0.001$.

proliferation (Fig. 6A and B). The effect of P-REX2a overexpression on cell cycle progression was measured by flow cytometry. The results showed that overexpression of P-REX2a induced A549 cells to reenter the S and G_2/M phases (Fig. 6C). Furthermore, P-REX2a overexpression eliminated the impact of miR-561 on A549 cell apoptosis (Fig. 6D). Overexpression of P-REX2a in A549 cells rescued the reduced P-REX2a mRNA expression levels induced by miR-561 (Fig. 6E). Further analysis revealed that compared with miR-561 overexpression, the overexpression of P-REX2a upregulated P-REX2a, p-AKT, cyclin D1, CDK2, and Bcl-2 protein expressions, and downregulated Bax and caspase 9/3 protein expressions (Fig. 6F). These findings further demonstrated that miR-561 plays a tumor suppressor role via the AKT signaling pathway by targeting P-REX2a.

DISCUSSION

In recent decades, emerging evidences have certified that miRNAs are actively involved in the pathogenesis

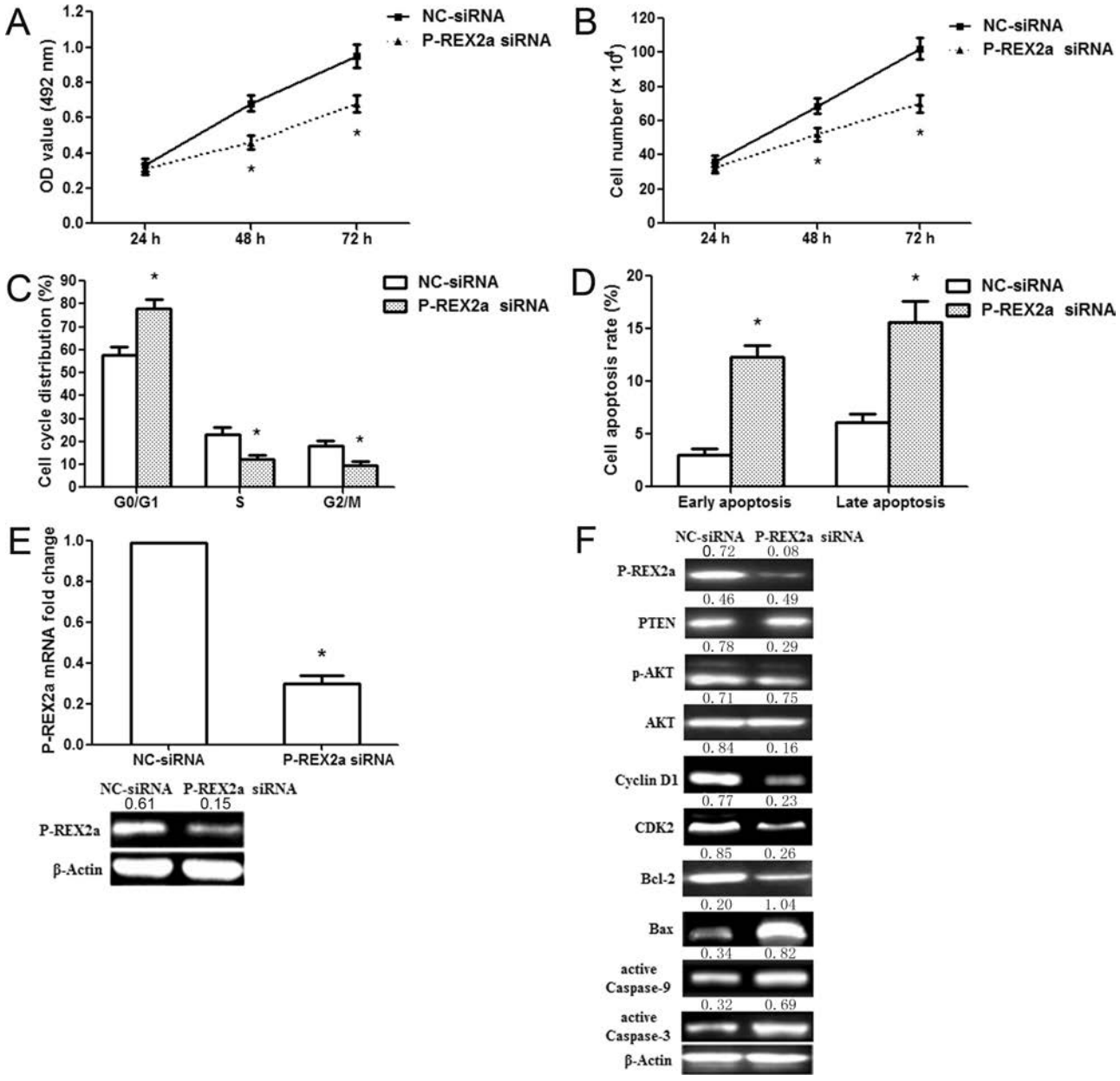

Figure 5. P-REX2a siRNA inhibits the proliferation of human NSCLC A549 cells. (A) P-REX2a siRNA decreased the activity of A549 cells at 48 and 72 h. (B) P-REX2a siRNA suppressed A549 cell proliferation. (C) Flow cytometric analysis showed the percentage of A549 cells in the G_0/G_1, S, and G_2/M phases. G_0/G_1 phase cells increased after P-REX2a siRNA treatment, and S and G_2/M phase cells were decreased. (D) The data showed the percentage of early and late apoptosis after P-REX2a siRNA treatment. (E) The knockdown efficiency of P-REX2a siRNA in A549 cells. (F) P-REX2a, p-AKT, cyclin D1, CDK2, Bcl-2, Bax, and caspase 9/3 protein expressions were examined after P-REX2a siRNA treatment. $*p < 0.01$.

of cancers[17]. Many miRNAs have been identified by microarray screening in NSCLC[18–20]. In addition, miRNAs have been found to be crucial regulators of NSCLC cell proliferation, survival, differentiation, apoptosis, metastasis, and invasion[21–24]. Due to the important roles of miRNAs in NSCLC, miRNAs have been proposed as prospective biomarkers and therapeutic targets of NSCLC[25]. Although the clinical significance of miRNAs has been well characterized in NSCLC, the functions and the underlying molecular mechanisms of dysregulated miRNAs remain unknown. Therefore, identifying miRNAs and elucidating their biological functions in NSCLC will help identify novel targets for diagnosis and therapy. Recent papers reported that miR-561 downregulated in

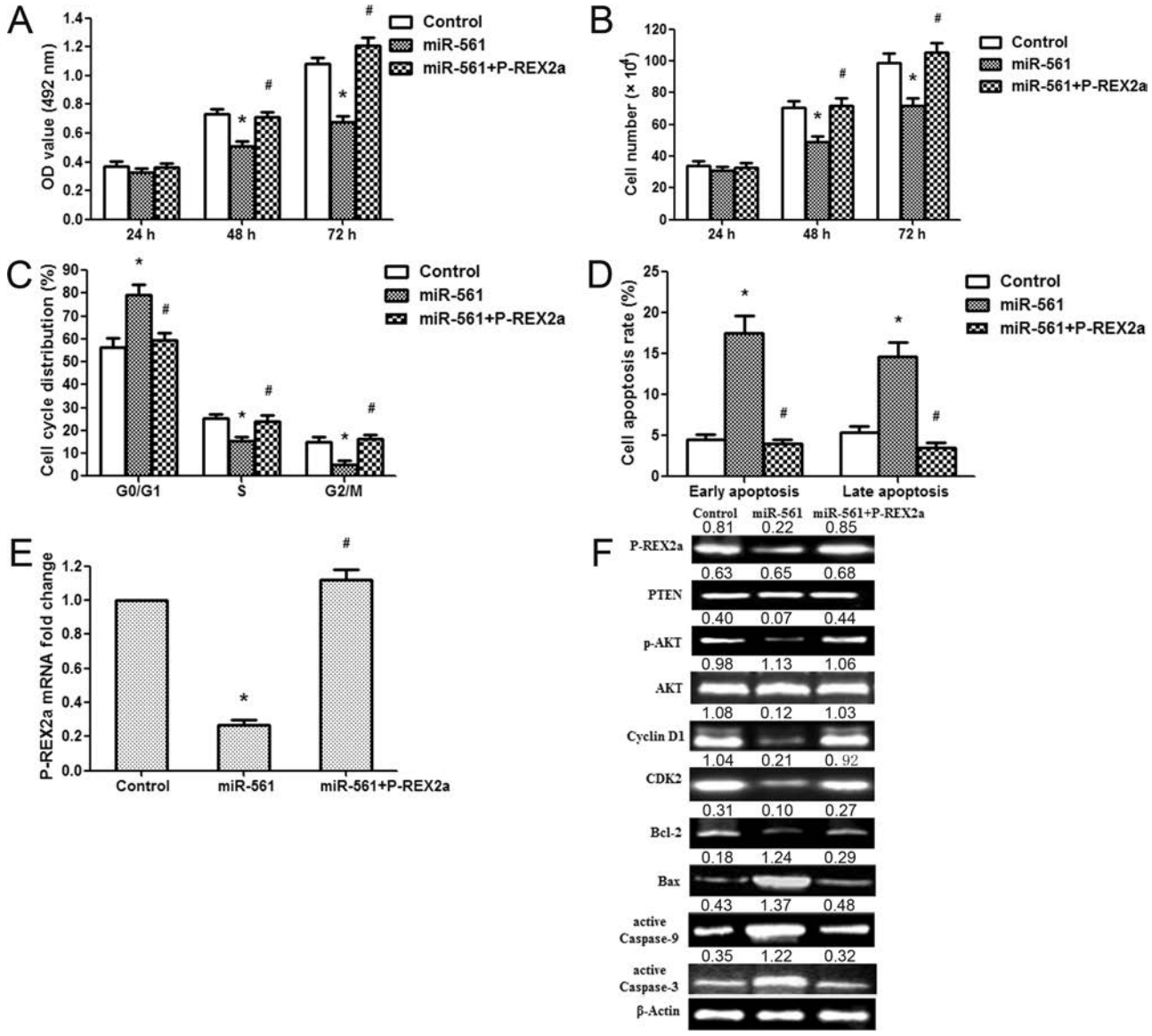

Figure 6. P-REX2a overexpression rescues miR-561-induced cellular phenotypes in NSCLC cells. (A) A549 cell activity was measured after cotransfection with P-REX2a and miR-561 vectors. (B) A549 cell proliferation was examined after cotransfection with P-REX2a and miR-561 vectors. (C) Cell cycle was determined in A549 cells at 48 h. (D) Apoptosis was detected in A549 cells at 48 h. (E) P-REX2a overexpression rescued P-REX2a mRNA expression levels reduced by miR-561. (F) P-REX2A, p-AKT, cyclin D1, CDK2, Bcl-2, Bax, and caspase 9/3 expressions were examined after cotransfection with P-REX2A and miR-561 vectors. *$p < 0.01$, compared with the vector control group; #$p < 0.01$, compared with the miR-561 overexpression group.

gastric cancer, and inhibited gastric cancer cell proliferation and invasion by downregulating c-Myc expression[15]. However, the exact functions and mechanisms of miR-561 during tumorigenesis in human NSCLC remain unclear. In this study, we found that miR-561 expression was dramatically downregulated in both NSCLC tissues and cell lines. The clinicopathological significance of miR-561 expression was also analyzed. The results showed that low miR-561 levels were significantly associated with TNM stage and tumor size in NSCLC patients, suggesting that miR-561 may play an importance role in NSCLC diagnosis. The experiments demonstrated that miR-561 overexpression remarkably inhibited NSCLC cell growth by inducing G_1/S phase arrest and promoted cell apoptosis, the inhibition of miR-561 facilitated cell proliferation and G_1/S transition and suppressed apoptosis. Our findings indicate that miR-561 plays a key role in NSCLC development and progression.

Moreover, our miR-561 target analysis identified P-REX2a as a direct target of miR-561. P-REX2a plays

crucial roles in regulating cell proliferation, differentiation, and apoptosis[16,26]. In this study, we found that P-REX2a was overexpressed in NSCLC compared with the level in normal tissues, which revealed an inverse correlation between P-REX2a mRNA expression and miR-561 expression in NSCLC tissues. These findings suggested that miR-561 might affect the progression of NSCLC by targeting NSCLC. Further bioinformatic analysis showed that there was an miR-561-binding site at 3,420–3,440 nt of the P-REX2a 3 -UTR. The dual-luciferase reporter assay verified that miR-561 directly targeted P-REX2a by recognizing the 3 -UTR of P-REX2a mRNA and inhibited P-REX2a translation. It is found that P-REX2a involves tumorigenesis and development. Evidence has demonstrated that P-REX2a plays an oncogenic role in breast cancer[16]. Furthermore, P-REX2a expression is increased in gastric cancer, and silencing of P-REX2a dramatically suppressed gastric cancer cell proliferation and induced apoptosis[26,27]. The findings also demonstrated that silencing of P-REX2a inhibited NSCLC cell proliferation by inducing G_1/S phase arrest and cell apoptosis. Moreover, we found that the overexpression of P-REX2a eliminated the tumor suppressor effect of miR-561 in NSCLC cells. Our results further verify that miR-561 functions as a tumor suppressor in NSCLC by suppressing P-REX2a expression.

P-REX2a regulates AKT phosphorylation in a PTEN-dependent manner by binding to PTEN. PTEN is a phosphatase that can dephosphorylate PIP3, the lipid product of the class I PI3K[28]. It is well known that PI3K/AKT signaling pathway is one of the most effective proliferation signaling pathways in cancers[29]. The abnormal AKT signaling pathway is involved in tumorigenesis and progression, such as gastric, liver, prostate, breast, and colorectal cancers[30]. It is found that the activation of AKT signaling pathway is associated with various clinicopathologic characteristics of cancer[31]. AKT regulates the function of generous substrates associated with cell cycle progression through direct phosphorylation of target proteins or indirectly controlling protein expressions[31]. Cyclin D1 and CDK2, AKT downstream regulators, are important transcriptional factors in the G_0/G_1 phase[32]. Cyclin A-CDK2 and cyclin D-CDK4/6 protein kinase complexes regulate the cellular progression from the G_1/G_0 phase to the S phase[33]. Some studies showed that cyclin D1 and CDK2 were involved in the human tumorigenesis[34]. The results demonstrated that miR-561 overexpression and P-REX2a siRNA could repress the cyclin D1 and CDK2 expressions and induce G_1/S phase arrest by inhibiting the AKT signaling pathway. In contrast, anti-miR-561 increased the expressions of cyclin D1 and CDK2, and drove more cells into the S and G_2/M phases through activation of the AKT signaling pathway. Furthermore, P-REX2a overexpression eliminated the effects of miR-561 overexpression on NSCLC cells. These findings suggest that miR-561 suppresses G_1/S phase transition via inhibition of the AKT signaling pathway by targeting P-REX2a.

Apoptosis is another crucial indicator for anticancer therapy. It is well known that mitochondria play important roles in apoptosis. The Bcl-2 family proteins, including either pro- or antiapoptotic activities, are shown to regulate apoptosis via mitochondria-associated apoptotic pathway. Antiapoptotic Bcl-2 protein inhibits apoptosis, while proapoptotic Bax protein activates apoptosis. An increased ratio of proapoptotic factors/antiapoptotic factors (Bax/Bcl-2) could result in the release of cytochrome c from mitochondria and activation of caspase 9 and caspase 3, which then induce apoptosis[35–38]. We provide evidence that miR-637-induced P-REX2a/AKT pathway plays a crucial role in the governance of the Bcl-2/Bax/caspase.

In summary, our study demonstrates that miR-561 functions as a tumor suppressor gene in NSCLC. We find that miR-561 is downregulated and associated with the clinicopathologic features of NSCLC patients. miR-561 inhibits NSCLC cell proliferation through suppression of the PTEN/AKT signaling pathway and induces apoptosis via regulation of Bcl-2/Bax/caspase expressions by targeting P-REX2a. These findings suggest that miR-561 plays a significant role in NSCLC progression and may serve as a potential novel target for NSCLC therapy.

ACKNOWLEDGMENTS: The present study was supported by Shaanxi Province Natural Science Foundation (No. 2017JM4358), Xi'an Municipal Science and Technology Project (No. 2017113SF/YX007(4)), and Youth Innovation Fund of the First Affiliated Hospital of Xi'an Jiaotong University (No. 2017QN-02). The authors declare no conflicts of interest.

REFERENCES

1. Torre LA, Siegel RL, Ward EM, Jemal A. Global cancer incidence and mortality rates and trends—an update. Cancer Epidemiol Biomarkers Prev. 2016;25(1):16–27.
2. Zhang WC, Chin TM, Yang H, Nga ME, Lunny DP, Lim EK, Sun LL, Pang YH, Leow YN, Malusay SR, Lim PX, Lee JZ, Tan BJ, Shyh-Chang N, Lim EH, Lim WT, Tan DS, Tan EH, Tai BC, Soo RA, Tam WL, Lim B. Tumour-initiating cell-specific miR-1246 and miR-1290 expression converge to promote non-small cell lung cancer progression. NAt Commun. 2016;7:11702.
3. Nguyen LV, Vanner R, Dirks P, Eaves CJ. Cancer stem cells: An evolving concept. Nat Rev Cancer 2012;12(2): 133−43.
4. Zhao L, Liu Y, Tong D, Qin Y, Yang J, Xue M, Du N, Liu L, Guo B, Hou N, Han J, Liu S, Liu N, Zhao X, Wang L, Chen Y, Huang C. MeCP2 promotes gastric cancer progression through regulating FOXF1/Wnt5a/beta-catenin and MYOD1/caspase-3 signaling pathways. EbioMedicine 2017;16:87–100.
5. Zhang J, Liu WL, Zhang L, Ge R, He F, G, Tian Q1, Mu X, Chen LH, Chen W, Li X. MiR-637 suppresses melanoma

progression through directly targeting P-REX2a and inhibiting PTEN/AKT signaling pathway. Cell Mol Biol. (Noisy-le-grand) 2018;64(11):50–7.
6. Liu L, Cui S, Zhang R, Shi Y, Luo L. MiR-421 inhibits the malignant phenotype in glioma by directly targeting MEF2D. Am J Cancer Res. 2017;7(4):857–68.
7. Zhao LY, Tong DD, Xue M, Ma HL, Liu SY, Yang J, Liu YX, Guo B1, Ni L, Liu LY, Qin YN, Wang LM, Zhao XG, Huang C. MeCP2, a target of miR-638, facilitates gastric cancer cell proliferation through activation of the MEK1/2-ERK1/2 signaling pathway by upregulating GIT1. Oncogenesis 2017;6(7):e368.
8. Ma Q, Wang Y, Zhang H, Wang F. miR-1290 contributes to colorectal cancer cell proliferation by targeting INPP4B. Oncol Res. 2018;26(8):1167–74.
9. Zhen Y, Liu J, Huang Y, Wang Y, Li W, Wu J. miR-133b inhibits cell growth, migration, and invasion by targeting MMP9 in non-small cell lung cancer. Oncol Res. 2017;25(7):1109–16.
10. Imbar T, Eisenberg I. Regulatory role of microRNAs in ovarian function. Fertil Steril. 2014;101(6):1524–30.
11. Jiang R, Zhang C, Liu G, Gu R, Wu H. MicroRNA-101 inhibits proliferation, migration and invasion in osteosarcoma cells by targeting ROCK1. Am J Cancer Res. 2017;7(1):88–97.
12. Wang X, Xu Y, Chen X, Xiao J. Dexmedetomidine inhibits osteosarcoma cell proliferation and migration, and promotes apoptosis by regulating miR-520a-3p. Oncol Res. 2018;26(3):495–502.
13. Dogini DB, Pascoal VD, Avansini SH, Vieira AS, Pereira TC, Lopes-Cendes I. The new world of RNAs. Genet Mol Biol. 2014;37(1):285–93.
14. Wang G, Fu Y, Liu G, Ye Y, Zhang X. miR-218 inhibits proliferation, migration, and EMT of gastric cancer cells by targeting WASF3. Oncol Res. 2017;25(3):355–64.
15. Qian K, Mao B, Zhang W, Chen H. MicroRNA-561 inhibits gastric cancer cell proliferation and invasion by downregulating c-Myc expression. Am J Transl Res. 2016; 8(9):3802–11.
16. Fine B, Hodakoski C, Koujak S, Su T, Saal LH, Maurer M, Hopkins B, Keniry M, Sulis ML, Mense S, Hibshoosh H, Parsons R. Activation of the PI3K pathway in cancer through inhibition of PTEN by exchange factor P-REX2a. Science 2009;325(5945):1261–5.
17. Tung SL, Huang WC, Hsu FC, Yang ZP, Jang TH, Chang JW, Chuang CM, Lai CR, Wang LH. miRNA-34c-5p inhibits amphiregulin-induced ovarian cancer stemness and drug resistance via downregulation of the AREG-WGFR-ERK pathway. Oncogenesis 2017;6(5):e326.
18. Li DY, Chen WJ, Luo L, Wang YK, Shang J, Zhang Y, Chen G, Li SK. Prospective IncRNA-miRNA-mRNA regulatory network of long non-coding RNA LINC00968 in non-small cell lung cancer A549 cells: A miRNA microarray and bioinformatics investigation. Int J Mol Med. 2017; 40(6):1895–906.
19. Tian W, Liu J, Pei B, Wang X, Guo Y, Yuan L. Identification of miRNAs and differentially expressed genes in early phase non-small cell lung cancer. Oncol Rep. 2016;35(4):2171–6.
20. Najafi A, Tavallaei M, Hosseini SM. A systems biology approach for miRNA-mRNA expression patterns analysis in non-small cell lung cancer. Cancer Biomark. 2016;16(1):31–45.
21. Cheng L, Zhan B, Luo P, Wang B. miRNA-375 regulates the cell survival and apoptosis of human non-small cell carcinoma by targeting HER2. Mol Med Rep. 2017;15(3):1387–92.
22. Jin X, Chen Y, Chen H, Fei S, Chen D, Cai X, Liu L, Lin B, Su H, Zhao L, Su M, Pan H, Shen L, Xie D, Xie C. Evaluation of tumor-derived exosomal mirna as potential diagnostic biomarkers for early-stage non-small cell lung cancer using next-generation sequencing. Clin Cancer Res. 2017;23(17):5311–9.
23. Ma Z, Cai H, Zhang Y, Chang L, Cui Y. MiR-129-5p inhibits non-small cell lung cancer cell stemness and chemoresistance through targeting DLK1. Biochem Biophys Res Commun. 2017;490(2):309–16.
24. Chi Y, Jin Q, Liu X, Xu L, He X, Shen Y, Zhou Q, Zhang J, Jin M. MiR-203 inhibits cell proliferation, invasion, and migration of non-small-cell lung cancer by downregulating RGS17. Cancer Sci. 2017; 108:2366–72.
25. Zhou Q, Huang SX, Zhang F, Li SJ, Liu C, Xi YY, Wang L, Wang X, He QQ, Sun CC, Li DJ. MicroRNAs: A novel potential biomarker for diagnosis and therapy in patients with non-small cell lung cancer. Cell Prolif. 2017;50(6).
26. Ai Y, Zhou Q, Li L, Pan Z, Guo M, Han J. Interference of P-REX2a may inhibits proliferation and reverse the resistance of SGC7901 cells to doxorubicin. Oncol Lett. 2018;15(3):3185–91.
27. Guo B, Liu L, Yao J, Ma R, Chang D, Li Z, Song T, Huang C. miR-338-3p suppresses gastric cancer progression through a PTEN-AKT axis by targeting P-REX2a. Mol Cancer Res. 2014;12(3):313–21.
28. Maehama T, Dixon JE. The tumor suppressor, PTEN/MMAC1, dephosphorylates the lipid second messenger, phosphatidylinositol 3,4,5-trisphosphate. J Biol Chem. 1998;273(22):13375–8.
29. Ejaz A, Mitterberger MC, Lu Z, Mattesich M, Zwierzina ME, Hörl S, Kaiser A, Viertler HP, Rostek U, Meryk A, Khalid S, Pierer G, Bast RC Jr, Zwerschke W. Weight loss upregulates the small GTPase DIRAS3 in human white adipose progenitor cells, which negatively regulates adipogenesis and activates autophagy via Akt-mTOR inhibition. EbioMedicine 2016;6:149–61.
30. Xu N, Lao Y, Zhang Y, Gillespie DA. AKT: A double-edged sword in cell proliferation and genome stability. J Oncol. 2012;2012:951724.
31. Zhang J, Tong DD, Xue M, Jiang QY, Wang XF, Yang PB, Ni L, Zhao LY, Huang C. FAM196B acts as oncogene and promotes proliferation of gastric cancer cells through AKT signaling pathway. Cell Mol Biol. (Noisy-le-grand) 2017;63(9):18–23.
32. Maddika S, Ande SR, Wiechec E, Hansen LL, Wesselborg S, Los M. Akt-mediated phosphorylation of CDK2 regulates its dual role in cell cycle progression and apoptosis. J Cell Sci. 2008;121(Pt 7):979–88.
33. Zhao LY, Zhang J, Guo B, Yang J, Han J, Zhao XG, Wang XF, Liu LY, Li ZF, Song TS, Huang C. MECP2 promotes cell proliferation by activation ERK1/2 and inhibiting p38 activity in human hepatocellular carcinoma HEPG2 cells. Cell Mol Biol. (Noisy-le-grand) 2013;59:OL1876–81.
34. Chu X, Zhang T, Wang J, Li M, Zhang X, Tu J, Sun S, Chen Z, Lu F. Alternative splicing variants of human Fbx4 disturb cyclin D1 proteolysis in human cancer. Biochem Biophys Res Commun. 2014;447(1):158–64.

35. Tamm I, Schriever F, Dorken B. Apoptosis: Implications of basic research for clinical oncology. Lancet Oncol. 2001;2(1):33–42.
36. Pieper AA, Verma A, Zhang J, Snyder SH. Poly (ADP-ribose) polymerase, nitric oxide and cell death. Trends Pharmacol Sci. 1999;20(4):171–81.
37. Czabotar PE, Lessene G, Strasser A, Adams JM. Control of apoptosis by the BCL-2 protein family: Implications for physiology and therapy, nature reviews. Mol Cell Biol. 2014;15(1):49–63.
38. Liu J, Huang R, Lin D, Peng J, Wu X, Lin Q, Pan XL, Song YQ, Zhang MH, Hou M, Chen F. Expression of survivin and bax/bcl-2 in peroxisome proliferator activate receptor-γ ligands induces apoptosis on human myeloid leukemia cells in vitro. Ann Oncol. 2005;16(3): 455–9.